Advanced Steel Construction – Vol. 18 No. 4 (2022) 804–817
DOI:10.18057/IJASC.2022.18.4.8

RETROFITTING COLLAPSE BEHAVIOR OF DOUBLE LAYER SPACE TRUSSES AGAINST PROGRESSIVE COLLAPSE BY FORCE LIMITING DEVICES

Saman Rashidyan [1, *] and Mohammad Reza Sheidaii [2]

[1] *Clinical Assistant Professor, Department of Mechanical Engineering, University of North Texas, 1155 Union Circle #305027, Denton, Texas 76203-5017*

[2] *Professor, Urmia University, Civil Engineering Department, Urmia University, West Azerbaijan Province, 24, Urmia Lake Bridge*

** (Corresponding author: E-mail: srashidyan@yahoo.com)*

ABSTRACT

Previous collapses of Double Layer Space Trusses (DLSTs) show that they are vulnerable to progressive collapse phenomenon. Under certain circumstances, a local failure can propagate throughout the structure and lead to occurring a brittle failure in the structure. Therefore, it is crucial to identify and exploit proper retrofitting methods against progressive collapse in DLSTs. In the current study, the method of utilizing Force Limiting Devices (FLDs) to improve the collapse behavior against progressive collapse have been investigated for flat DLSTs with overall collapse and dynamic snap-through. The results show that introducing FLDs to the critical members of the top layer of a flat DLST with dynamic snap-through failure mode and a member imperfection of 0.005L provides 18.2 to 23.86% load bearing increase and ductility between 1.55 to 1.67. The results also show that when the DLSTs is made of members with geometric imperfections between 0.001 L and 0.004 L, the FLDs can convert the overall collapse of the DLSTs to a ductile collapse. For this member imperfection range, the obtained data show that the method can increase the load bearing capacity of the models from 18.35to 26.8% and provide ductility between 1.56 to 1.76. The provided ductility in models with smaller member imperfection is slightly greater than those provided in models with larger member imperfection. In the current study the activation level of FLDs are selected between 85 to 95 percent and the effect of FLD activation level is also investigated. In addition, the results showed that placing FLDs on critical members could provide a ductility significantly greater than the ductility provided by another method of retrofitting DLSTs called the method of over designing the members of compression layer and under designing the members of tension layer.

ARTICLE HISTORY

Received: 13 September 2020
Revised: 20 July 2021
Accepted: 22 July 2021

KEYWORDS

Force limiting device;
Double layer space truss;
Progressive collapse;
Snap-through;
Buckling

1. Introduction

Double Layer Space Trusses (DLSTs) are among proper structures to cover large areas since their stiffness and load bearing capacity are high due to their efficient geometry. In general, these structures collapse in one of the modes shown in Fig. 1. In the 'overall collapse' mode, when a member buckles the distribution of the load happens quickly; therefore, the rest of the structure is not able to hold the distributed load and the structure will collapse after the first set of members fail. In the 'local collapse along with dynamic snap-through' the load shedding by the failure of compression member occurs abruptly, however, the rest of the structure can hold the load which is distributed. In this case, the buckling of this first of members will result in a large change in displacement. For cases in which the released energy is enormous, other members may not be able to absorb the excessive released energy and consequently the structure collapses due to the large released energy. The chain of the failures occurring in such cases is called a progressive collapse phenomenon. In contrast, in 'local collapse without dynamic snap-through', the load distribution occurs gradually; therefore, no additional dynamic load distribution is generated in such collapse modes.

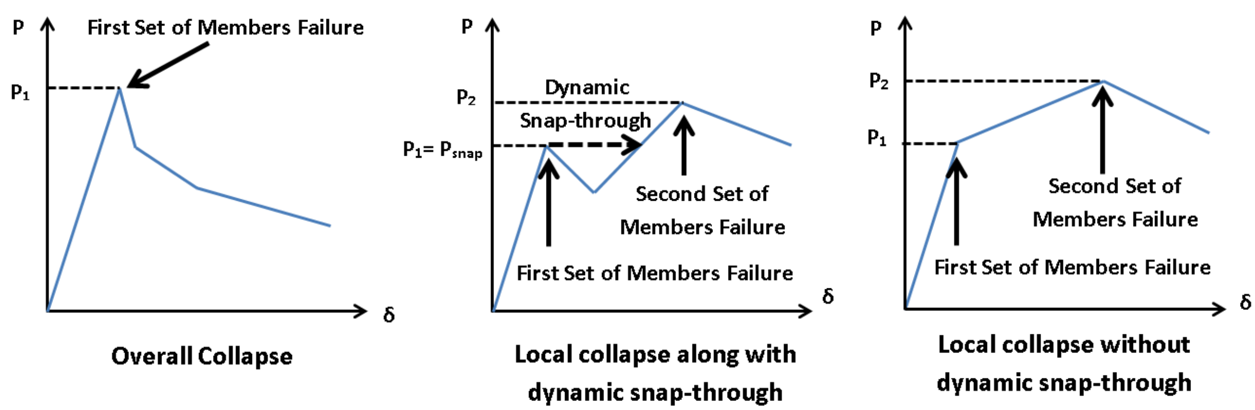

Fig. 1 Collapse modes in DLSTs

The collapse form of the DLSTs can be identified using a static collapse analysis. Since the failure behavior of the DLSTs is highly dependent on the behavior of the constituting members, the behavior of the tensile and compression members should be determined in the first step. In tensile members, when load increases, the stress reaches to the yielding stress. At this time, the member does not collapse, and it still can carry loads due to its strain hardening behavior. This behavior continues with large strains until the member ruptures. In contrast, the load bearing capacity reduction usually occurs in a brittle manner in members under compression forces. Even in trusses where yielding occurs in tension members, the failure is finally dictated by the buckling of the compression members [1–3]. Under common slenderness ratios, the buckling of a compression members is brittle in most of the cases [4].

After completing the static analysis if the obtained graphs show the occurrence of snap-through in the DLST, a dynamic snap-through analysis is done to determine the real strength of the structure during the occurrence of progressive collapse [5]. Many references show the necessity of considering the dynamic effects of progressive collapse in trusses [6] and frame structures [7–9]. It should be noted that when dynamic snap-through happens in the structure, conducting a dynamic analysis is necessary in such cases to obtain a realistic behavior of the structure.

After completing the failure analysis of the DLST, if the results show the occurrence of 'overall collapse' or 'local collapse along with dynamic snap-through', appropriate methods should be used to improve the behavior of the DLST against the brittle failure in such structures.

One proper method is over designing the members of the top layer along with under designing the members of bottom layer. In this method the tension members yield before the compression members buckle. This delays the failure of the compression members and consequently a good level of ductility will be provided [4]. A comprehensive study regarding this method is conducted by Rashidyan and Sheidaii [10].They used this method on five DLST models with various conditions. They showed that 30%-40% overdesign of all top and under design of bottom members results in satisfactory ductility level and load bearing capacity in their investigated models.

The method of using Force Limiting Devices (FLD) to change the brittle behavior of members under compression to a ductile behavior is another proper method to enhance the collapse behavior of DLSTs. These devices have a rigid-plastic behavior and are installed on selected critical compression members of the DLST. The load under which the devises start working is slightly less than the load under which the member buckles. This load level will be kept constant even when the load on structure increases. Therefore, a compression member protected by an FLD would have an elastic-plastic behavior rather than a brittle behavior.

The theoretical benefits of FLDs were first shown by Schmidt and Hanaor [11] and results of some prototype devices were demonstrated by Hanaor and Schmidt [12]. To investigate the ability of the FLDs in enhancing the collapse behavior of the DLSTs, Hanaor et al. [4] tested Bamford and Mero shaped DLSTs with FLDs and the results were compared to trusses with no devices. The DLSTs equipped with FLDs withstood up to 23% higher than the control truss, with considerably enhanced ductility. Parke [13] showed the effectiveness of a devised FLD system indicated in Fig. 2 on the collapse behavior of space trusses. His devised FLD system consists of tubes and strips as indicated in Fig. 2. When a compressive load is applied on the member, both tubes subject to compression whereas the strips are under tension forces. If the system is designed such that the strips yield prior to the failure of the tubes, the overall behavior of the member would be ductile as can be seen in Fig.2b.

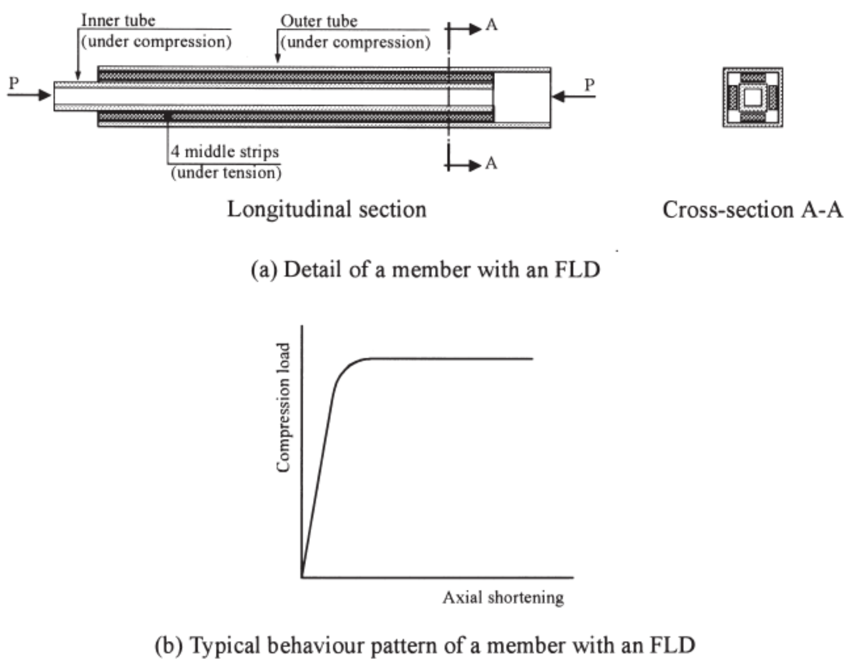

Fig. 2 (a) Detail of a member with an FLD and (b) typical modified behavior pattern [13]

El-Sheikh [14] showed the influence of FLDs on the behavior of 3-D trusses through a parametric study on trusses with overall and local collapse without dynamic snap-through. He investigated the effect of both the location and number of the compression members with FLDs on the ductility level and strength of the space trusses. His studies revealed that, using FLDs on top chord members that are under largest stresses can improve the overall behavior and strength of the DLSTs with overall and local collapse without dynamic snap-through. The method could also improve the ductility of his investigated space trusses. Bai and Zhang [15] presented the performance of FLDs on roof trusses under combined static and transient wind loading. Kim and Chae [16] studied 'out of plane' type, 'slit' type and 'folded plate' type FLDs and showed the effectiveness of such devices using experimental and numerical methods. Poursharifi et al. [17] introduced an Accordion Force Limiting Device (AFLD). They studied their proposed AFLD under compressive forces and showed that the AFLD could modify the brittle behavior of the members. Abedi and Kolachahi [18] applied FLDs on double-layer barrel vault space structures. Their results demonstrated the efficiency of the FLDs in preventing progressive collapse. The influence of FLDs on tensegrity structures has also been investigated by Shekastehband [19]. He showed that using FLDs in critical members can lead to a ductile behavior and increases the strength of the investigated tensegrity structures up to 52%.

In the above-mentioned investigations, the applicability of the method in improving the collapse behavior of various DLSTs, double-layer barrel vaults and tensegrity structures has been demonstrated. However, the performance of FLDs on flat DLSTs with dynamic snap-through collapse has not been discussed in the literature. Since the large released snap-through energy can have an important adverse impact on the collapse behavior of the DLSTs it was decided to see how the FLDs affect the collapse behavior of such structures. In addition, there is still a need to reveal more aspects of the performance of FLDs on flat DLSTs with overall collapse and the effect of important factors such as member imperfection and FLDs activation level should be scrutinized. Thus, this study first tries to investigate how FLDs can enhance the collapse behavior of flat DLSTs where dynamic snap-through occurs. Second, DLSTs with overall collapse behavior having different member imperfection and FLD activation level are analyzed to examine the effect of such factors on the effectiveness of using FLDs. In the end, the results of this study were also compared to another retrofitting method called the method of over designing the members of compression layer and under designing the members of tension layer to improve the collapse behavior of flat DLSTs suggested by Rashidyan and Sheidaii [10]. Since the DLST models used in both studies are the same, the comparison of the results can help obtaining more insight regarding the effectiveness of installing FLDs on DLSTs. Also, we would like to acknowledge that the analysis method that we have utilized in this paper has previously been used and verified in several studies [5,10,20,21].

2. Parametric study

2.1. Investigated models

Five flat square on square offset DLST [22] models are initially investigated in this research. The initial models were selected with various support conditions, member imperfection, structure height and plan shapes in order to investigate the impact of such leading factors on the failure behavior of DLSTs. The investigated models are also the same as the ones used by Rashidyan and Sheidaii [10]. This let the research team compare some results from applying the FLDs on the DLST models with the results obtained from the method of over designing the members of compression layer and under designing the members of tension layer. The characteristics of the DLST models are shown in Table 1. The geometry of Models G1 to G5 is shown in Fig. 3. Pin supports were used in all the models. The pin supports were located only at the four corners of the bottom layer for models G1 to G4. However, Model G5 has pin supports at all the 32 bottom joints located on the external perimeter.

Table 1
Characteristics of investigated models [10]

Model	Length (m)	Width (m)	h(m)	Geometrical imperfection of members	Supports location
G1	9.6	9.6	0.75	0.001 L[a]	Corner nodes of bottom layer
G2	9.6	9.6	0.75	0.005 L	Corner nodes of bottom layer
G3	9.6	9.6	0.5	0.001 L	Corner nodes of bottom layer
G4	9.6	7.2	0.75	0.001 L	Corner nodes of bottom layer
G5	9.6	9.6	0.75	0.001 L	All bottom layer external nodes

[a] Length of member

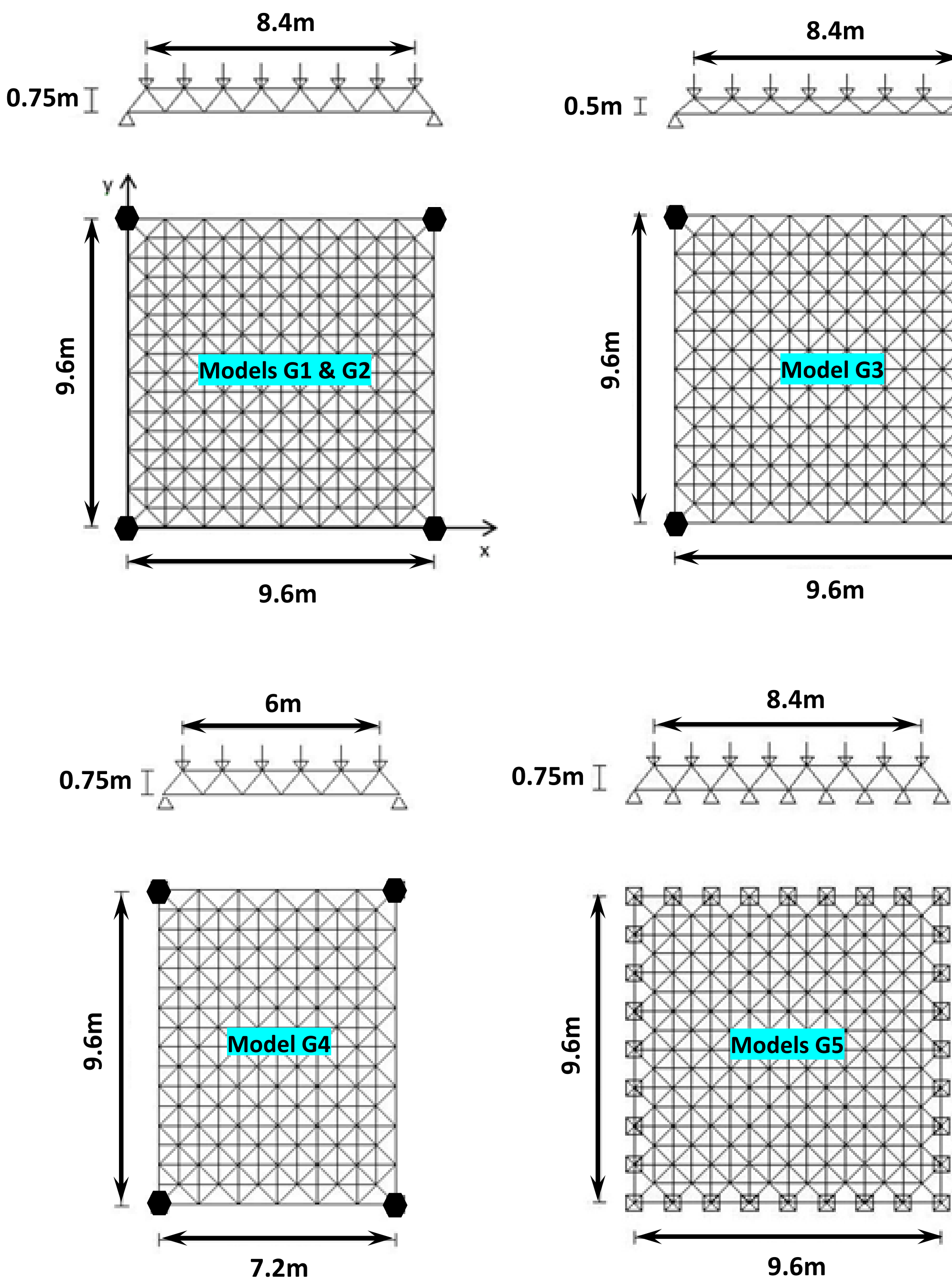

Fig. 3 Geometry of Models G1 to G5

2.2. Design of the investigated models

The steel DLSTs were analyzed and designed using SAP 2000 software [23]. To do so the dead and snow loads indicated in Table 2 were applied on the DLSTs according to ASCE/SEI 7-1[24]. In order to transfer the snow loads to the structure, a flat sandwich panel cover was considered at the top of the DLST. The dead loads from the weight of the roof cover and from the weight of the DLST members have been distinguished in Table 2. The yielding stress and the modulus of elasticity were assumed 240 and 210000 MPa respectively.

Table 2
Assumed dead and snow loads in models G1 to G5

Model	Dead load due to the weight of roof cover (Kgf/m^2)	Dead load from the weight of members of the DLST (Kgf/m^2)	Snow Load (Kgf/m^2)
G1	70	38	100
G2	70	38	100
G3	70	46	100
G4	70	25	100
G5	70	15	100

In the next step the uniform dead and snow loads were multiplied by the tributary area of the top joints of the DLST and the product was applied at the top joints as concentrated loads and the DLSTs were analyzed. After analyzing the structures, the DLST members were designed in accordance to AISC 360-16 [25]. Identical steel hollow-circular cross sections were utilized for all the members. Solid members were used at the corners in Models G1 to G4 though. The characteristics of the chords used in each model are shown in Table 3.

Table 3
Characteristics of chords in G1 to G5 [10]

Model	Member	External diameter (mm)	Thickness (mm)	Slenderness ratio	Geometrical imperfection
G1	P1	48	5.6	79	0.001 L*
G2	P2	48	5.6	79	0.005 L
G3	P3	89	3.6	40	0.001 L
G4	P4	57	2.9	63	0.001 L
G5	P5	38	2.6	96	0.001 L

*Member's length

2.3. Collapse behavior of the investigated models

As stated earlier, a static analysis needs to be done to determine the failure mode of the DLST models. The behavior of the tensile and compression members was determined using finite element method. In this research LUSAS software [26] was used to determine the behavior of the members and collapse behavior of the DLSTs.
Following assumptions [5] were assumed for the finite element analysis:

- The material has an Elasto-plastic behavior.
- The members are pined at the two ends.
- Kirchhoff thin beam elements are used.
- 10 finite elements were considered for each member.
- Nonlinear behavior pertaining to materials and geometry are considered.
- Intrinsic geometrical imperfections are considered by assuming a pre-made curvature as indicated in Fig. 4. Maximum geometrical imperfection (Δ) exists at the middle of the member.

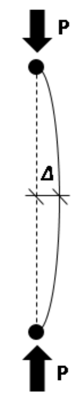

Fig. 4 Hinge-end compression member with initial curvature (geometrical imperfection)

Considering the abovementioned assumptions, the curves indicated in Fig. 5 were obtained for members P1 to P5.

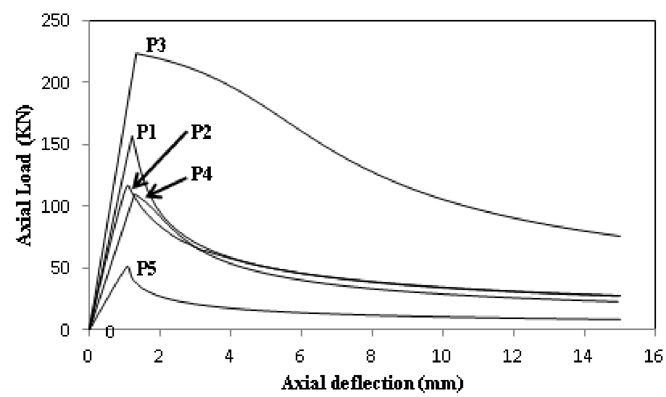

Fig. 5 Axial force-deformation curves for P1 to P5 [10]

After determining the load deformation of the members, their stress-strain behavior graphs were obtained using piece-wise linearization method [27]. The stress-strain curves for P1 to P5 are shown in Fig. 6. Theses graphs in addition to 2-node truss elements were used to perform the failure analysis of the DLST models. This strategy can remarkedly reduces time especially in large DLSTs.

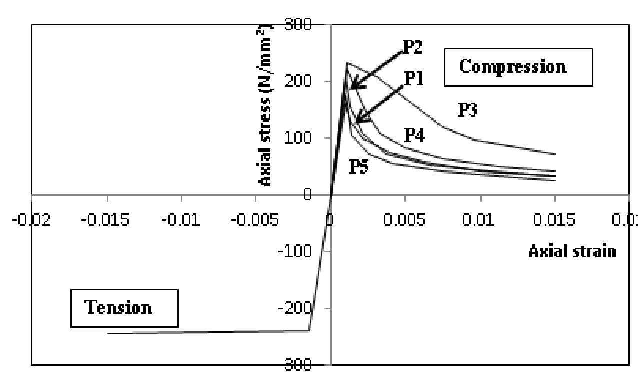

Fig. 6 Stress-strain curves for members P1 to P5 [10]

After determining the behavior of the members, nonlinear static collapse analysis was performed on the DLST models G1 to G5. In the nonlinear static analysis, the matrix form of the equilibrium of the structure is as follows:

$$KD = P \tag{1}$$

where K, D, and P are the stiffness matrix, displacement vector and load vector respectively. After conducting the nonlinear static analysis on Models G1 to G5, the load deflection curves of the node located at the center of the top layer of each model are obtained and shown in Fig. 7.

The graphs shown in Fig. 7 indicate that the failure mode in models G1, G3, G4 and G5 is an overall collapse. However, a local failure accompanied with dynamic snap-through takes place in Model G2. The first set of failure in model G2 happens at 4782 N (which is P_{snap}) and the maximum load bearing capacity is achieved at 5232 N. The P_{snap} (Point 1) and maximum load bearing capacity of Model G2 are shown on the load deflection diagram of the node located at the center of the top layer in Fig. 8. The state of the structure at Point 2 is also called a 'configuration strain' state.

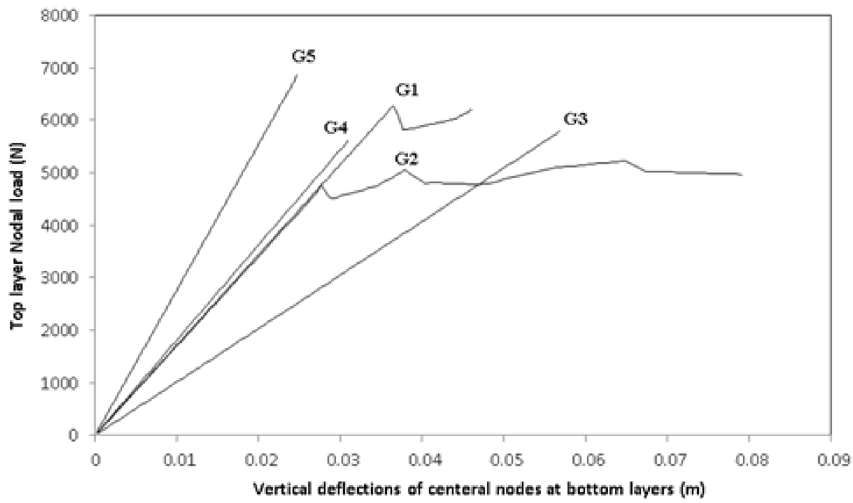

Fig. 7 Load deflection curves of nodes located at the center of top layer of models G1 to G5 [10]

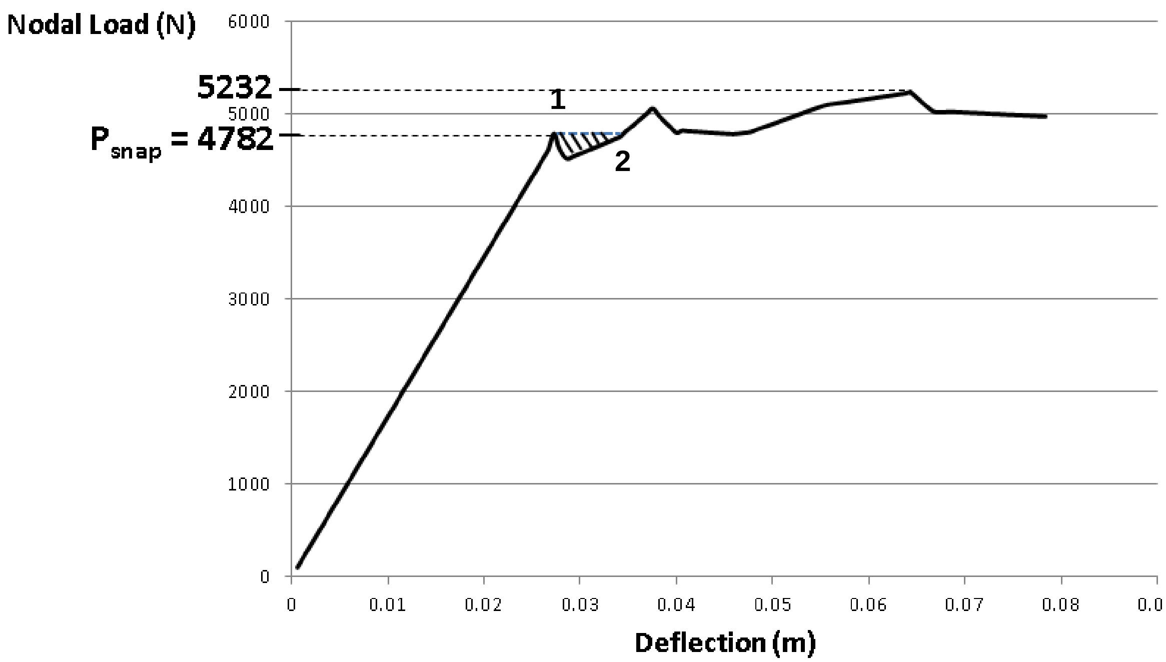

Fig. 8 Load deflection curve of the node located at the center of the top layer in model G2 [10]

Although the maximum load bearing capacity of Model G2 is obtained as 5232 N, the actual value may be smaller due to the released energy during the dynamic snap-through phenomenon. Thus, a dynamic snap-through analysis should be done at this time.

Among various dynamic methods, the energy method was selected and utilized in this study since it is a proper method to evaluate the dynamic behavior of DLSTs [20]. The energy method was performed according to the following procedure.

The matrix form of the static equilibrium of the structure was indicated in Equation 1. By gradually increasing the applied load in the static analysis, the structure will approach a state point where snap-through occurs. Assuming that the snap through happens at a load level of P_{snap}, the equilibrium equations at the time of snap-through will be:

$$K_{snap} D_{snap} = P_{snap} \tag{2}$$

where D_{snap} is the static displacement at the time of snap-through and K_{snap} is its corresponding stiffness matrix. When structure reaches to this point, snap-through takes place and accordingly a huge energy is released since some compression members buckle. The released energy can now be expressed as the sum of kinetic energies corresponding to nodal snap-through of all loaded nodes. The kinetic energy corresponding to the nodal snap-through of a loaded node can be obtained by measuring the area bounded between the load deflection curve and a horizontal line drawn from P_{snap}. The shaded area corresponding to the released energy at the node located at the center of the top layer of Model G2 is indicated in Fig. 8.

Based on the abovementioned discussion, the kinetic energy was determined for all top loaded nodes of Model G2 using the load deflection diagrams of the top nodes. Due to symmetry, only the diagrams of ten top layer loaded nodes of Model G2 are shown in Fig. 9. The locations of the nodes are also indicated on Fig. 10.

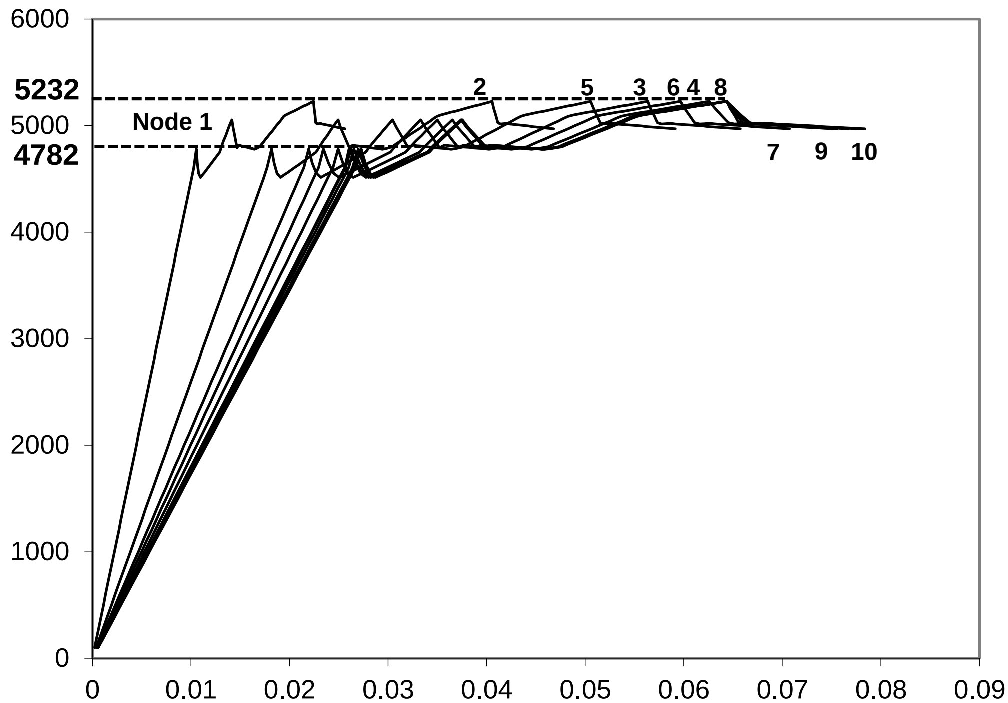

Fig. 9 The load deflection graphs of ten top layer loaded nodes of Model G2

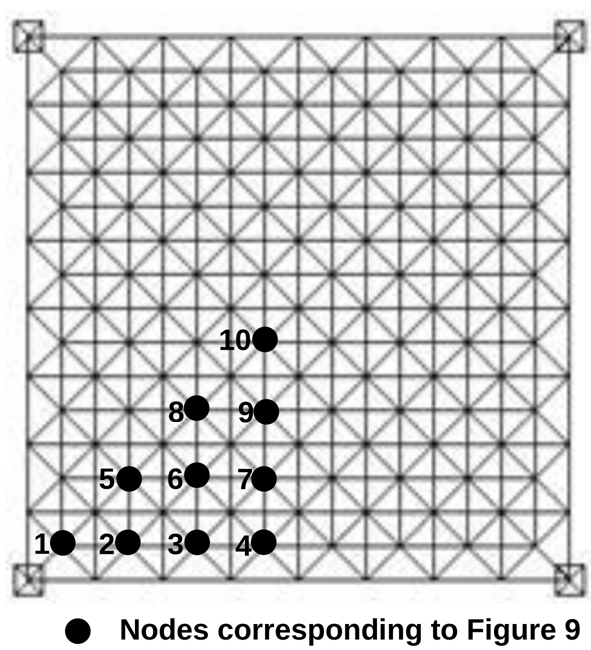

Fig. 10 Ten loaded nodes of the top layer of Model G2

Table 4
calculated kinetic energies and their corresponding velocities for ten nodes of Model G2 indicated in Fig. 10

Node	U (N.m)	*v* (m/s)
1	12.30	0.225
2	23.45	0.310
3	34.90	0.378
4	40.70	0.409
5	29.85	0.350
6	35.40	0.381
7	38.35	0.400
8	36.05	0.385
9	36.55	0.387
10	35.70	0.383

After computing the kinetic energies, the associated velocities at the abovementioned nodes are determined with the help of Equation 3. The calculated energies and their associated velocities for the ten nodes of Model G2 shown in Fig. 10 are summarized in Table 4.

$$v = \sqrt{\frac{2Ug}{P_{snap}}} \tag{3}$$

U: Shaded area
g: acceleration of gravity (m/s^2)

In the next step a nonlinear eigen value analysis is performed and the natural frequencies of the models were calculated. The Rayleigh coefficients can then be calculated and used to obtain the damping matrix using mass matrix M and stiffness matrix K as follows:

$$C = \alpha_m M + \beta_s K \tag{4}$$

α_m and β_s are the mass and stiffness proportional damping coefficients. In order to determine Rayleigh coefficients, the natural frequencies of the first five modes of the vibration of the structures should be obtained from the eigen value analysis. In DLSTs, the damping ratios of the first and fifth modes (ζ_1 and ζ_5) can be assumed 1.5 % and 2.5% respectively[28]. Thus, the Rayleigh coefficients can be calculated as:

$$\alpha_m = 2\omega_1\omega_5(\xi_1\omega_5 - \xi_5\omega_1)/(\omega_5^2 - \omega_1^2) \tag{5}$$
$$\beta_s = 2(\xi_5\omega_5 - \xi_1\omega_1)/(\omega_5^2 - \omega_1^2)$$

where w_1 and w_5 are the natural frequencies of the first and fifth modes respectively.

Considering the above-mentioned procedure, the natural frequencies and Rayleigh coefficients of Model G2 are calculated and shown in Table 5.

Table 5
Natural frequencies and Rayleigh coefficients of Model G2

Model	w_1 (hz)	w_5 (hz)	α_m	β_s
G2	58.12	171.53	0.8575	0.0001623

In the final step, a dynamic nonlinear analysis is conducted to determine the dynamic response to snap-through. This analysis is performed on the strain configuration of the structure (Point 2 in Fig. 8) considering both geometric and material nonlinearities. In order to do this dynamic analysis, the strain configuration becomes subjected to the load P_{snap} and nodal velocities calculated previously. In this case, considering the initial conditions:

$$M\ddot{D}_d + C\dot{D}_d + K(D_d + D_{snap}) = P_{snap} \tag{6}$$

where M, C and K are dependent on static deflection D_{snap} and dynamic deflection D_d. By solving this equation of motion, the time-history graphs for each node can be obtained.

The time-history graph of the deflection of the node located at the middle of the top layer of Model G2, is shown in Fig. 11. This graph shows that progressive collapse occurs in Model G2 since the deformation is getting larger significantly. Thus, the actual maximum load is 4782 N which is 9.4 percent smaller than the one determined from the static failure analysis (5232N).

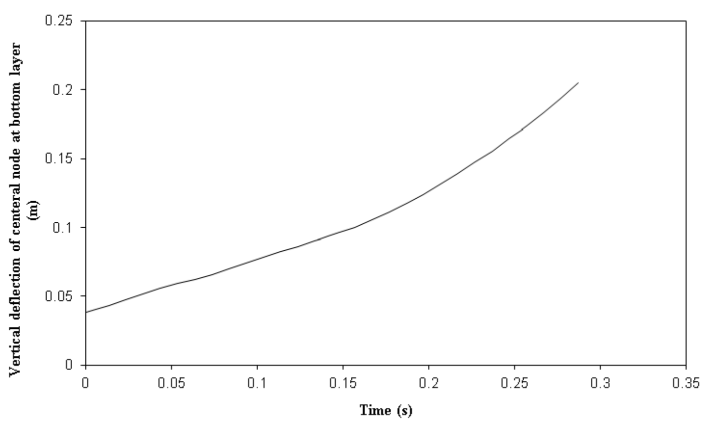

Fig. 11 Deflection curve obtained at the node located at the center of the bottom layer of Model G2 [10]

Since the results of the collapse analysis show that Model G2 has a brittle behavior due the occurrence of to snap-through, suitable methods should be utilized to convert its brittle collapse to a ductile collapse. The method of utilizing FLDs to achieve this goal is considered and explained in the next section.

2.4. Discussion of Utilizing Force Limiting Devices (FLDs) Method on Models

2.4.1. Results of applying FLDs on the top layer members of Models G1 to G5

In this section, first the effect of FLDs on the ductility and strength of Model G2 with dynamic snap-through collapse is investigated. All the members of Model G2 are P2 rods (see Table 2). The FLDs that are introduced to the members are activated when the axial load of the member P2 reaches to 85 percent of its failure load. The data of Fig. 5 shows that the failure load of member P2 is 117 kN. Therefore, the activation level of its introduced FLD is set on 99.5 kN which is 85 percent of 117kN. The axial load-deflection graphs of the member P2 and its introduced FLD are shown in Fig. 12.

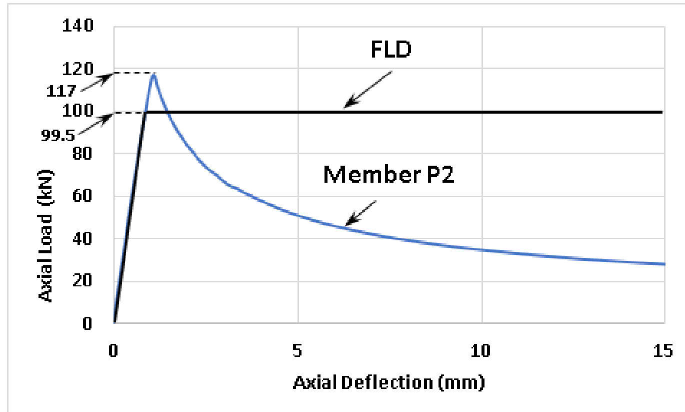

Fig. 12 Axial load-deflection of member P2 and its introduced FLD

It should be noted that FLDs are expensive devices. Therefore, they should only be installed on selected critical members. In order to identify the most critical members of the structure, the FLDs were first installed on all the members of the top layer to see which members have already been activated at the time of the collapse of Model G2. Those members then would be considered critical compression members. Placing the FLDs on all the top members not only helps identifying the critical members but also disclose the maximum ideally achievable load bearing capacity and ductility, without limiting the number of the FLDs to only critical members of the top layer.

The vertical load-displacement graphs of the original (without FLD) and modified Model G2 (with FLD on all top members) is depicted in Fig. 13. The location of the critical members in which the FLDs have been activated are shown in Fig. 14. The results of collapse analysis of modified and initial Model G2 are summarized in Table 6. In this table the ductility (μ) is computed using Equation 2.

$$\mu = \frac{\delta_u}{\delta_1} \tag{2}$$

δ_u: Ultimate deflection
δ_1: Deflection corresponding to first failure

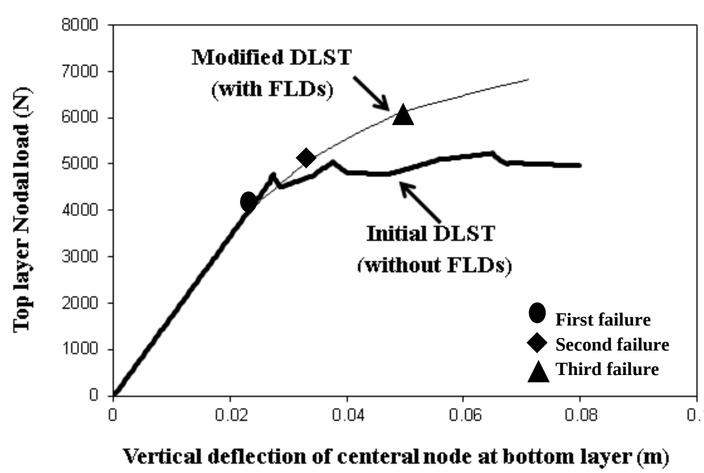

Fig. 13 Vertical load-displacement graphs of initial and modified Model G2

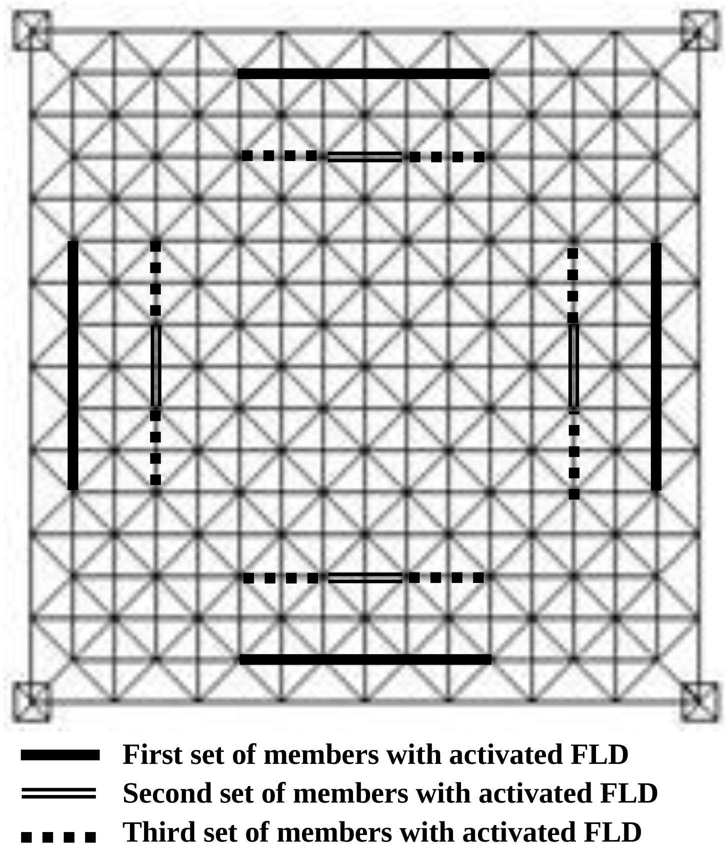

Fig. 14 Location of the critical members in which the FLDs have been activated

Table 6
Results of collapse analysis of modified DLST model G2

Maximum Load Bearing Capacity of Original DLST (N)	Maximum Load Bearing Capacity of Modified DLST (N)	Load Bearing Capacity Increase (%)	Ultimate Deflection in Central Node of Modified DLST (cm)	Central Node Deflection Corresponding to First Failure in Modified DLST (cm)	Ductility
4782	6824	42.7	7.10	2.41	2.95

The curves shown in Fig. 13 demonstrate that a significant ductility can be achieved by using FLDs on top layer members of the Model G2. While the FLDs are activated at %85 of the load bearing capacities of the members, Model G2 does not fail and it can withstand excessive plastic deformations without being collapsed. Model G2 collapses when the central node deflections reached 2.95 times of the deflection corresponding to the first failure occurred in the structures. The results of Table 6 also show that using FLDs on top layer members can increase the load bearing capacity of Model G2 by 42.7 percent. Thus, the method not only alters the collapse behavior from brittle local collapse with dynamic snap-through to a ductile type, but also significantly increases the strength of the structure.

Before discussing the effect of placing FLDs on the critical members of Model G2 it was decided to see if similar observations can be made from models with different conditions and collapse behavior. Therefore, the FLDs were introduced to all top members of Models G1, G3, G4 and G5 with overall collapse and different imperfection, support condition, and shape. The vertical load-displacement graphs of the initial and modified Models G1, G3, G4 and G5 are shown in Fig. 15. The results of the analysis are also summarized in Table 7.

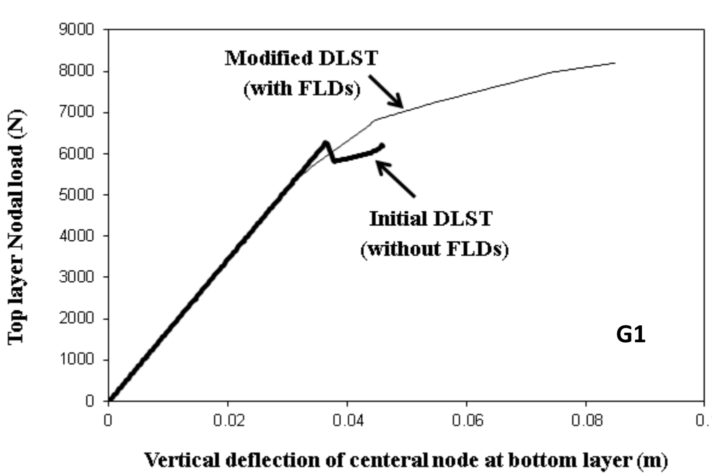

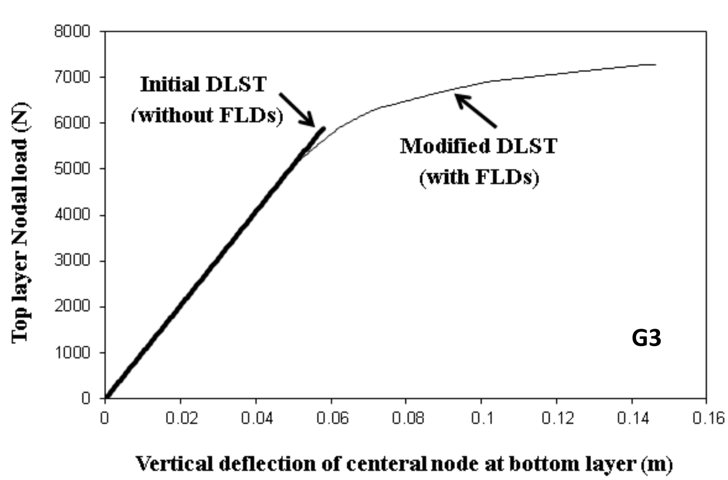

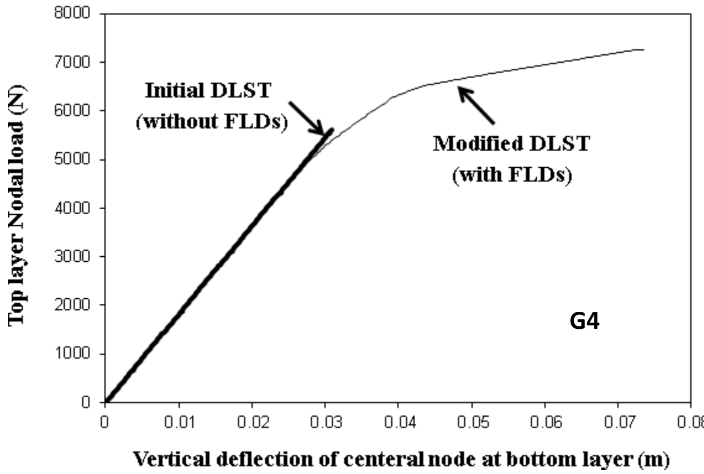

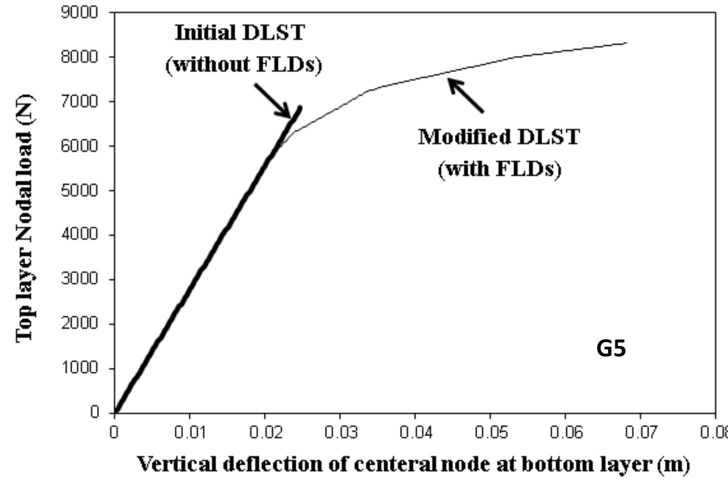

Fig. 15 Vertical load-displacement graphs of initial and modified Models G1, G3, G4 and G5

Table 7
Summary of the collapse analysis of modified DLST models G1, G3, G4 and G5

Model	Maximum Load Bearing Capacity of Original DLST (N)	Maximum Load Bearing Capacity of Modified DLST (N)	Load Bearing Capacity Increase (%)	Ultimate Deflection in Central Node of Modified DLST (cm)	Central Node Deflection Corresponding to First Failure in Modified DLST (cm)	Ductility
G1	6279	8200	30.6	8.49	3.02	2.81
G3	5794	7284	25.7	14.61	4.94	2.98
G4	5613	7266	29.4	7.35	2.63	2.80
G5	6875	8304	20.8	6.80	2.05	3.32

The graphs indicated in Fig. 15 show that a considerable ductility can be achieved by using FLDs on top layer members of the DLST models. The model with supports located at the corners shows the best results with maximum ductility of 3.317. Similar to Model G2, utilizing FLDs converts a brittle collapse into a ductile failure in the investigated models with overall collapse. The results of Table 7 show that using FLDs on the top members can increase the load bearing capacity of the models from 20.8 to 30.6 percent which are less than the capacity increase values in the Model G2 with dynamic snap through. In summary, the method can convert the collapse behavior from brittle overall collapse and snap through to a ductile failure as well as increase the strength of the structures.

2.4.2. Comparing the Results of applying FLDs on the top layer members of Models G1 to G5 with the method of overdesigning top members with undersigning bottom layer members

Here the abovementioned conclusions are compared to the results obtained from the study conducted by Rashidyan and Sheidaii [10]. As indicated previously, Rashidyan and Sheidaii [10] used the method of overdesigning the compression members with undersigning the bottom layer members of flat DLSTs to improve the collapse behavior of such structures. They showed that 30%-40% overdesign of all top and under design of bottom members would result in satisfactory ductility and load bearing capacity in models G1 to G5. The results of their study and the current study are compared in Table 8.

Table 8
The results of study performed by Rashidyan and Sheidaii (2017) and Tables 6 and 7

Model	Load Bearing Capacity Increase (%)			Produced Ductility		
	Using FLD	30% Over and under design	40% Over and under design	Using FLD	30% Over and under design	40% Over and under design
G1	30.6	10.9	7.7	2.8	1.4	1.7
G2	42.7	17.5	18.5	2.95	1.0	1.2
G3	25.7	5.3	3.2	2.98	1.38	1.81
G4	29.4	14.02	11.33	2.80	1.48	1.92
G5	20.8	11.81	5.63	3.32	1.37	1.84

The results indicated in Table 8 show that the method of using FLD on all top members can provide more load bearing capacity increase and ductility compared to the method studied by Rashidyan and Sheidaii [10] in all the investigated models.

2.4.3. Results of applying FLDs on critical top layer members of Model G2 with various member imperfection and FLD activation level

In this section, Model G2 is focused again to investigate the effect of introducing FLDs on critical members of the top layer. The analysis was performed with three various activating levels of 85, 90 and 95 percent of the load bearing capacity of the members. The critical members of Model G2 are indicated in Fig. 14. As stated previously, the critical members have been obtained from the results of collapse analysis when all the top members are equipped with FLDs. At the time of failure of Model G2, the FLDs had been activated in the critical members shown in Fig. 14 which were the most highly stressed members of the top layer. The number of the critical members in Model G2 is approximately 5 percent of all the top layer members.

The vertical load-displacement graphs of the original (without FLD) and modified models equipped with FLD are depicted in Fig. 16a. The results reported by Rashidyan and Sheidaii [10] are also indicated in Fig. 16b for comparison. The results of the comparison of the two methods are summarized in Table 9.

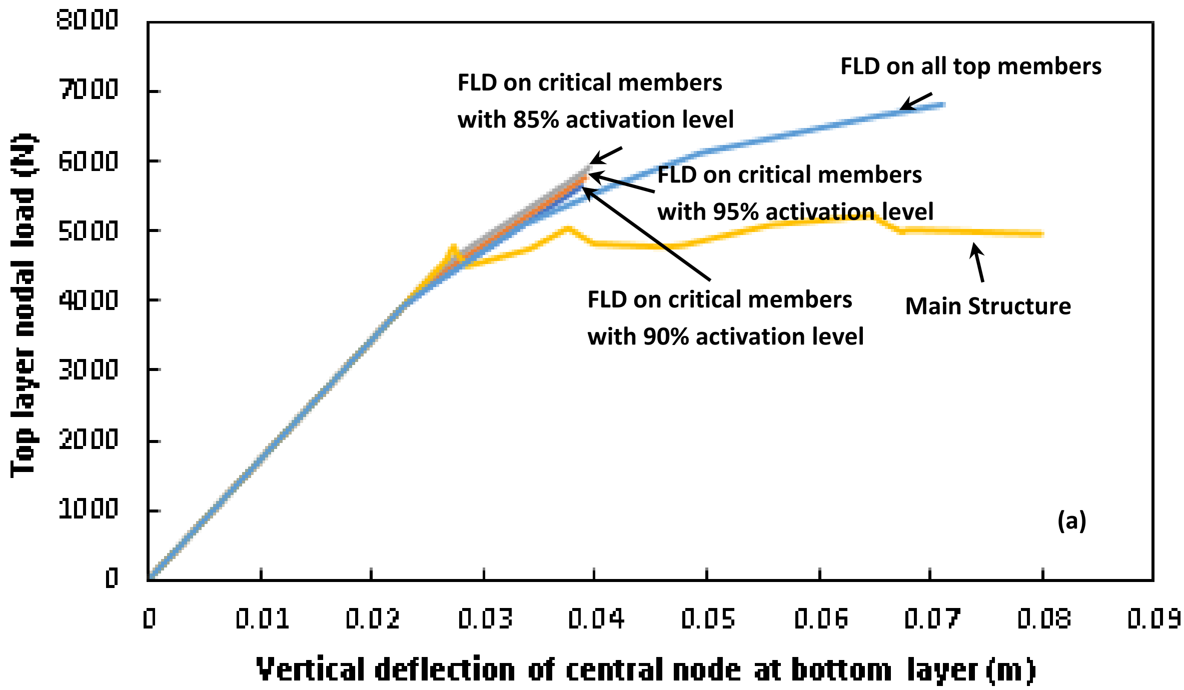

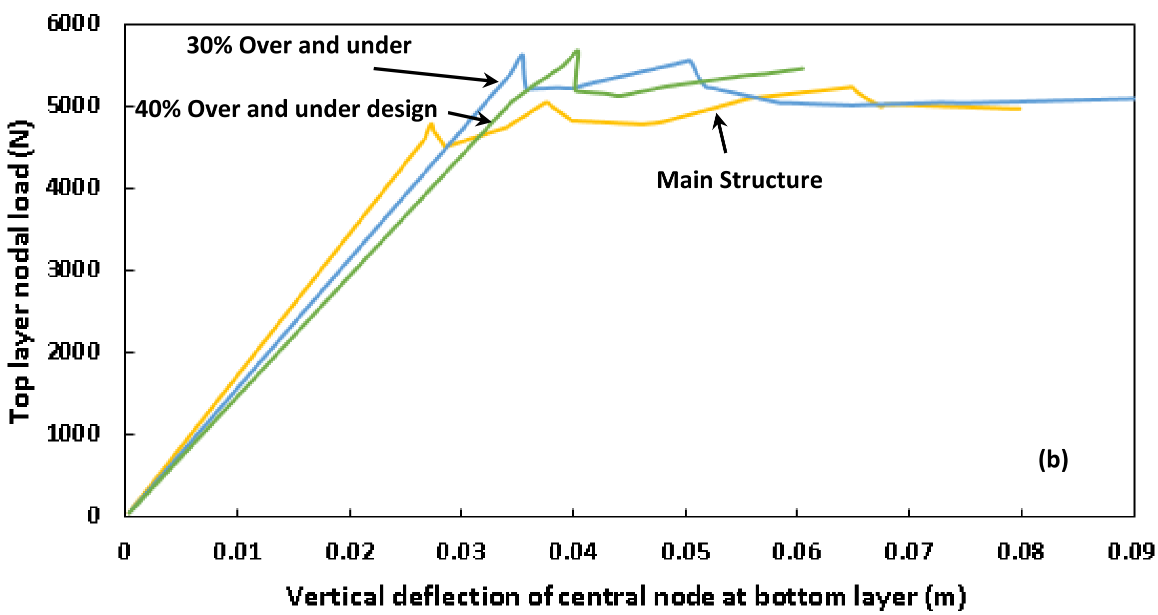

Fig. 16 (a) Vertical load-displacement graphs of the original (without FLD) and modified models with FLD activation levels pertaining to 85%, 90% and 95% of the bucking load of compression members (b) vertical deflection of central node vs. top layer nodal load for model G2 when top members are overdesigned and under designed by 30% and 40%.

Table 9
Collapse analysis summary for modified DLST model G2

Improving Method	Maximum Load Bearing Capacity of Original DLST (N)	Maximum Load Bearing Capacity of Modified DLST (N)	Load Bearing Capacity Increase (%)	Ultimate Deflection in Central Node of Modified DLST (cm)	Central Node Deflection Corresponding to First Failure in Modified DLST (cm)	Ductility
FLDs on all top members	4782	6824	42.7	7.10	2.41	2.95
FLDs on critical members with 85% activation limit		5651	18.20	3.88	2.27	1.67
FLDs on critical members with 90% activation limit		5776	20.79	3.91	2.41	1.62
FLDs on critical members with 95% activation limit		5923	23.86	3.94	2.53	1.55
30% Under and over design		5619	17.50	3.55	3.55	1
40% Under and over design		5669	18.55	4.04	3.41	1.18

The results indicated in Table 9 shows that applying FLDs on critical members provides 18.2 to 23.86% load bearing increase values which are close to those provided by the method presented by Rashidyan and Sheidaii (2017). The load bearing capacity of the model increases when the activation level become greater. The data indicated in Table 9 also shows that the ductility provided by placing the FLDs on critical members is between 1.55 to 1.67 which is significantly greater than 1 and 1.18 that are obtained from Rashidyan and Sheidaii [10]. Although all three levels of 85, 90 and 95 percent result in a considerable ductility, the achievable ductility become greater when the activation level of the FLDs is lower. The data of Table 9 shows that the ductility obtained from 85 percent activation level is 3.1 and 7.7 percent greater than those obtained from 90 and 96 percent respectively.

In addition to the effect of activating levels of the FLDs, it was decided to examine the effect of various member imperfections in Model G2. The member imperfections 0.001 to 0.004L and FLD activation levels of 85, 90 and 95% were considered. Models G2-1, G2-2, G2-3, and G2-4 have the same geometry as Model G2 but member imperfections equal to 0.001L, 0.002 L, 0.003L, and 0.004 L respectively. After assigning the FLDs to the critical top members of Models G2-1, G2-2, G2-3, and G2-4, the collapse analyses were carried out. It should be noted that the critical members have been identified using the same procedure which was mentioned previously for Model G2. The vertical load-displacement graphs of the original (without FLD) and modified models (with FLD) are shown in Fig. 17. The conclusions are indicated in Table 10.

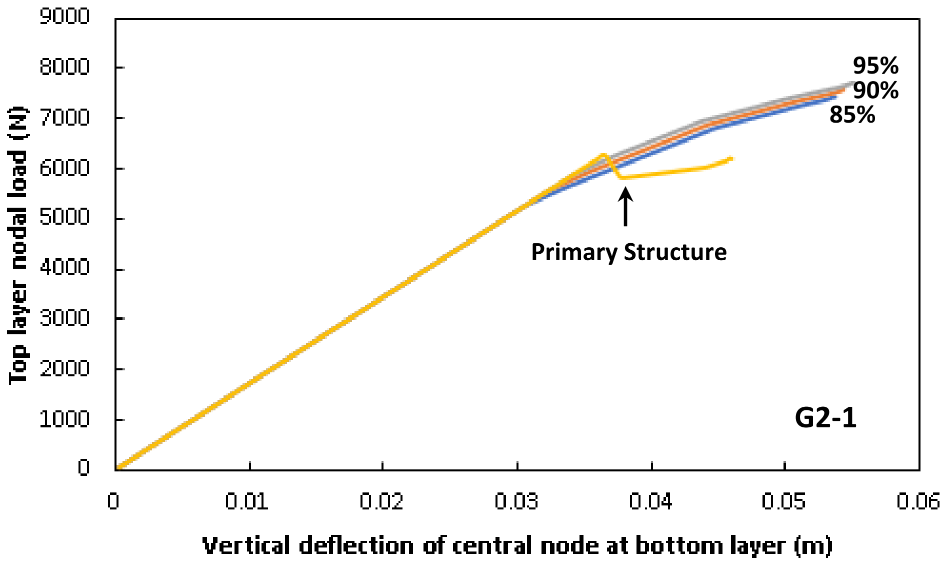

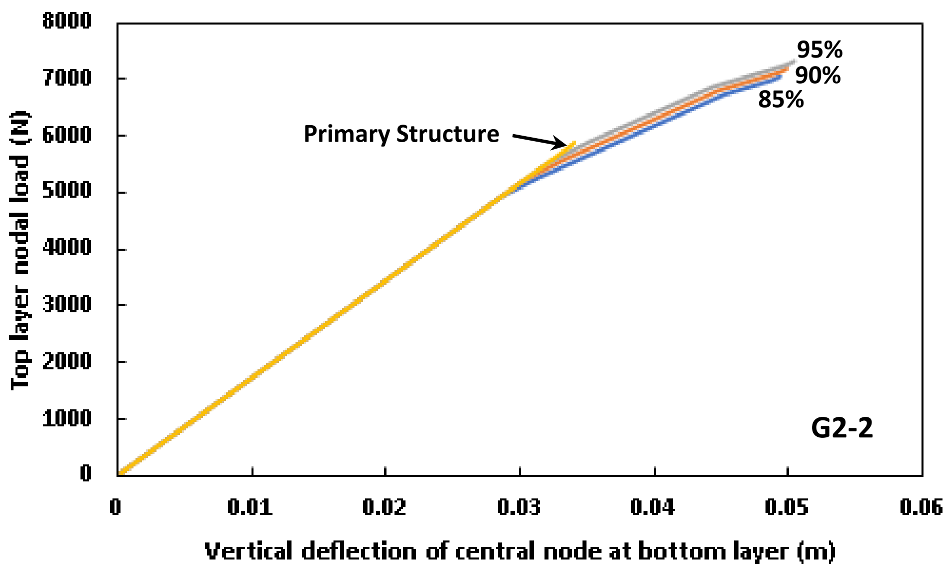

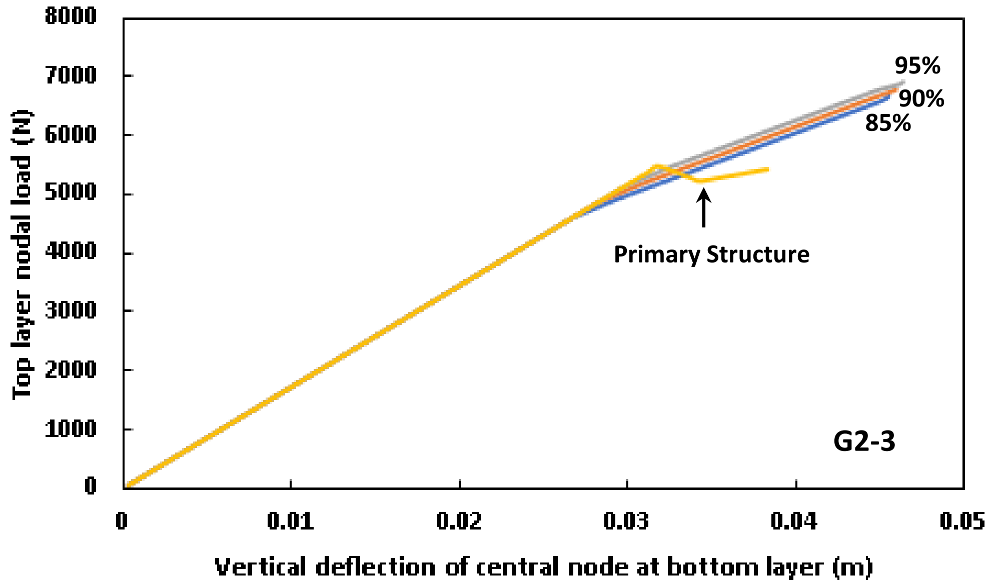

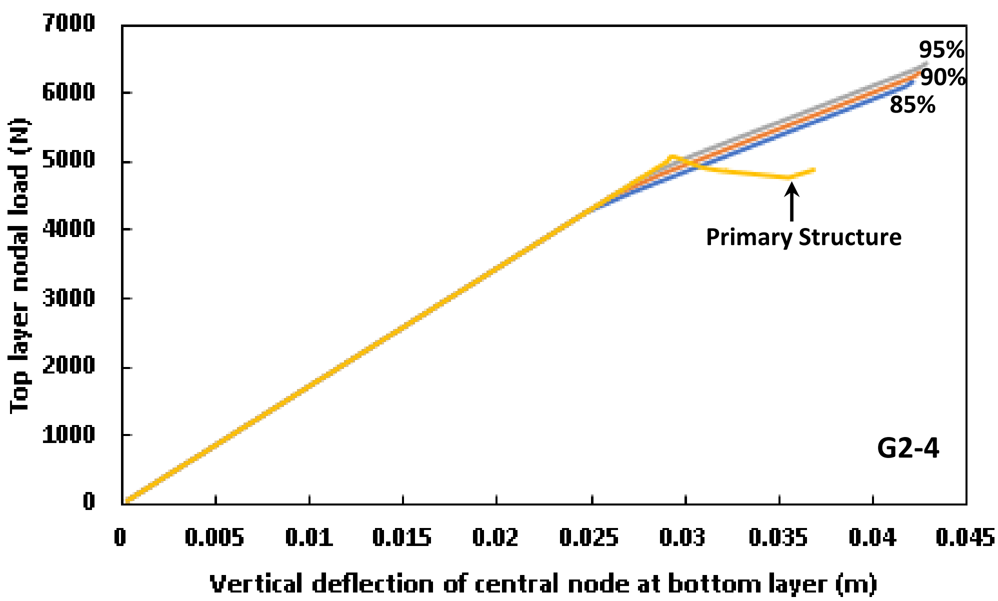

Fig. 17 Vertical load-displacement graphs of the primary (without FLD) and modified Models G2-1, G2-2, G2-3, and G2-4 with various activation levels

Table 10
Collapse analysis summary of modified DLST models G2-1, G2-2, G2-3 and G2-4

Model	Member Imperfection	FLD Activation Limit Percent	Maximum Load Bearing Capacity of Original DLST (N)	Maximum Load Bearing Capacity of Modified DLST (N)	Load Bearing Capacity Increase (%)	Ultimate Deflection in Central Node of Modified DLST (cm)	Central Node Deflection Corresponding to First Failure in Modified DLST (cm)	Ductility
G2-1	0.001 L	85	6279	7431	18.35	5.37	3.05	1.76
		90		7571	20.58	5.43	3.25	1.67
		95		7708	22.76	5.51	3.43	1.61
G2-2	0.002 L	85	5879	7050	19.92	4.93	2.82	1.75
		90		7188	22.27	4.98	3.02	1.65
		95		7306	24.27	5.03	3.17	1.59
G2-3	0.003 L	85	5478	6670	21.76	4.55	2.67	1.71
		90		6782	23.80	4.60	2.84	1.62
		95		6910	26.14	4.64	2.96	1.58
G2-4	0.004 L	85	5079	6169	21.46	4.21	2.47	1.70
		90		6285	23.74	4.24	2.61	1.62
		95		6440	26.80	4.29	2.76	1.56

First the curves shown in Fig. 17 show that when the imperfections of the members are changed from 0.005 L in Model G2 to imperfections between 0.001 L and 0.004 L in Models G2-1 to G2-4, the collapse modes are not dynamic snap-through anymore. They are overall collapse, instead. Second, the curves shown in Fig. 17 show that the method of applying FLD on critical members can convert the brittle collapse to a ductile collapse for all models with imperfections between 0.001 L and 0.004 L. The results indicated in Table 10 shows that the method can increase the load bearing capacity of the models between 18.35 to 26.8%. The provided ductility of the modified models is between 1.54 to 1.74 which shows a significant ductility. These ranges of increase in load bearing capacity and ductility are very close to those obtained from model G2 with dynamic snap through. The data of Table 10 also shows that the provided ductility in models with smaller member imperfection is slightly greater than those provided in models with larger member imperfection. In addition, the ductility provided by FLDs with various levels of activation looks different based on data indicated in Table 10. A comparison of the ductility obtained from activation levels of 85, 90 and 95 is demonstrated in Table 11. The data of Table 11 shows that the achievable ductility from FLDs with activation level of 85 percent is 4.9 to 6.1 and 8.2 to 10.1 greater than those obtained from 90 and 95 percent respectively. Therefore, an activation level of 85 percent has superiority over 90 and 95 percent. The activation level of 85 percent has two more advantages. First, it has a reasonable clearance with respect to the failure load of the member which leads to more safety. This clearance assures that the FLD is activated before the member reaches to its failure load. Second his level is far enough from the level of service loads and it won't be activated on slight variations of the service loads.

Table 11
Comparison of ductility obtained from activation levels of 85, 90 and 95percent

(1) Model	(3) Ductility (%85 activation level)	(4) Ductility (90% activation level)	(5) Ductility (95% activation level)	(6) $\frac{(3)-(4)}{(4)} \times 100$	(7) $\frac{(3)-(5)}{(5)} \times 100$
G2-1	1.76	1.67	1.61	5.4	9.3
G2-2	1.75	1.65	1.59	6.1	10.1
G2-3	1.71	1.62	1.58	5.6	8.2
G2-4	1.70	1.62	1.56	4.9	9.0

In summary, the presented results show that the method of applying FLDs on the critical members of the DLSTs not only can provide ductility to the structures with dynamic snap-through but also can increase the ductility and load bearing capacity when the imperfection of the members are between 0.001 L and 0.005 L and the activation level of the FLDs is between 85 and 95 percent.

3. Conclusion

The method of using FLDs on critical members of the DLSTs is a proper method to improve the collapse behavior of these structures against progressive collapse. In the current study, first the critical members of a DLST were identified and the FLDs were installed on them. Then the collapse analysis was performed with three different FLD activation levels. The results showed that applying FLDs on critical members provided 18.2 to 23.86% load bearing increases and ductility values between 1.55 to 1.67. The results were compared with the method of overdesigning the top compression members with undersigning the bottom layer tension members of flat DLSTs. The FLD method was then applied on four DLSTs with the same geometry but made of members with different geometrical imperfections. The results showed that when the imperfections of the members in the unequipped models were changed from 0.005 L to values between 0.001 L and 0.004 L the collapse modes were converted to overall collapse from a risky dynamic snap-through mode. The results also showed that the method of applying FLD on critical members could convert a brittle overall collapse to a ductile collapse for all models with imperfections between 0.001 L and 0.004 L. The obtained data showed that the method could increase the load bearing capacity of the models between 18.35 and 26.80%. The ductility of the models was also obtained withing the range of 1.56 and 1.7. The data also confirmed that the provided ductility in models with smaller member imperfection was slightly greater than those provided in models with larger member imperfection. In addition, the comparison of the ductility obtained from FLD activation levels of 85, 90 and 95 showed that the achievable ductility from FLDs with activation level of 85 percent is 4.9 to 6.1 and 8.2 to 10.1 greater than those obtained from 90 and 95 percent respectively. Therefore, an activation level of 85 percent showed superiority over 90 and 95 percent in providing ductility for the structure. The activation level of 85 percent, however, has two more advantages. First, it has a reasonable clearance with respect to the failure load of the member which result in more safety for the entire structure. This clearance assures that the FLD is activated before the member reaches to its failure load. Second his level is far enough from the level of service loads and it won't be activated on slight variations of the service loads. In summary, the presented results show that the method of applying FLDs on the critical members of the DLSTs not only can provide significant ductility to the structures with dynamic snap-through and overall collapse but also can increase the load bearing capacity when the imperfection of the members are between 0.001 L and 0.005 L and the FLDs activation level is set between 85 to 95 percent.

References

[1] L. Schmidt, K. Cogan, P. Morgan, A. Omeagher, Ultimate load behaviour of a full scale space truss., Proceedings of the Institution of Civil Engineers. 69 (1980) 97–109.

[2] L.C. Schmidt, P. Morgan, A. Hanaor, Ultimate load testing of space trusses, Journal of the Structural Division. 108 (1982).

[3] C. Vatansever, Investigation of buckled truss bars of a space truss roof system, Engineering Failure Analysis. 106 (2019).

[4] A. Hanaor, C. Marsh, G.A.R. Parke, Modification of Behavior of Double-Layer Grids: Overview, Journal of Structural Engineering. 115 (1989) 1021–1037.

[5] M.R. Sheydaii, A. K, B. A.a.d, P. G.a.r, An investigation into the collapse behaviour of double-layer space trusses, 27 (2003) 0–0.

[6] R.B. Malla, P. Agarwal, R. Ahmad, Dynamic analysis methodology for progressive failure of truss structures considering inelastic postbuckling cyclic member behavior, Engineering Structures. 33 (2011) 1503–1513.

[7] M. Ferraioli, Dynamic increase factor for pushdown analysis of seismically designed steel moment-resisting frames, Int J Steel Struct. 16 (2016) 857–875.

[8] Y. Li, X. Lu, H. Guan, P. Ren, Numerical investigation of progressive collapse resistance of reinforced concrete frames subject to column removals from different stories, Advances in Structural Engineering. 19 (2016) 314–326.

[9] A.Ch. Salmasi, M.R. Sheidaii, Assessment of eccentrically braced frames strength against progressive collapse, Int J Steel Struct. 17 (2017) 543–551.

[10] S. Rashidyan, M.-R. Sheidaii, Improving double-layer space trusses collapse behavior by strengthening compression layer and weakening tension layer members, Advances in Structural Engineering. 20 (2017) 1757–1767.

[11] L.C. Schmidt, A. Hanaor, Force Limiting Devices in Space Trusses, Journal of the Structural Division. 105 (1979) 939–951.

[12] A. Hanaor, L.C. Schmidt, Space Truss Studies with Force Limiting Devices, Journal of the Structural Division. 106 (1980) 2313–2329.

[13] G.A.R. Parke, A novel soft member for space-trusses, in: SPACE STRUCTURES 4, VOL 1, UNIV SURREY, GUILDFORD, ENGLAND, 1993: pp. 116–126.

[14] A. El-Sheikh, Effect of force limiting devices on behaviour of space trusses, Engineering Structures. 21 (1999) 34–44.

[15] L. Bai, Y. Zhang, Nonlinear dynamic behavior of steel framed roof structure with self-centering members under extreme transient wind load, Engineering Structures. 49 (2013) 819–830.

[16] C.H. Kim, W.T. Chae, A Study on the Development of Force Limiting Devices of Cross-Section Cutting Types, Journal of Korean Society of Steel Construction. 27 (2015) 77–85.

[17] M. Poursharifi, K. Abedi, M. Chenaghloua, 05.32: Experimental and numerical study on the collapse behavior of an all-steel accordion force limiting device, Ce/Papers. 1 (2017) 1315–1324.

[18] K. Abedi, S.R. Kolachahi, Investigation into the double-layer barrel vault space structure resistance to progressive collapse, Proceedings IRF2018: 6th International Conference Integrity-Reliability-Failure, Lisbon, Portugal. (2018).

[19] B. Shekastehband, The influences of force-limiting devices and high-stiffness cables on behavior of tensegrity structures, Arch Appl Mech. 88 (2018) 2293–2316.

[20] K. Abedi, M.R. Sheidaii, Investigation of Double-layer Grid Space Structurer Resistance to Progressive Collapse, Computational Methods in Engineering. 26 (2007) 149–164.

[21] M.R. Sheidaii, G.A.R. Parke, K. Abedi, A. Behravesh, Dynamic snap-through buckling of truss-type structures, International Journal of Space Structures. 16 (2001) 85–93.

[22] G.S. Ramaswamy, M. Eekhout, Analysis, Design and Construction of Steel Space Frames, Thomas Telford, 2002.

[23] SAP 2000, Computers and Structures Inc., Berkeley, CA.

[24] Minimum Design Loads and Associated Criteria for Buildings and Other Structures (ASCE/SEI 7-16), American Society of Civil Engineers, Reston, Virginia, USA.
[25] Specification for Structural Steel Buildings (ANSI/AISC 360-16) | American Institute of Steel Construction,
[26] LUSAS, Surrey, UK.
[27] M.R. Sheidaii, S. Gholizadeh, An investigation into the collapse behavior of double-layer space truss using neural networks, in: 7th International Congress on Civil Engineering, 2006.
[28] K. Abedi, G.A.R. Parke, Progressive Collapse of Single-Layer Braced Domes, International Journal of Space Structures. 11 (1996) 291–306.